International Journal of Mass Spectrometry 275 (2008) 80–85

Contents lists available at ScienceDirect

International Journal of Mass Spectrometry

journal homepage: www.elsevier.com/locate/ijms

Recombination of KrD^+ and XeD^+ ions with electrons

R. Plasil*, I. Korolov, T. Kotrik, J. Glosik

Department of Surface and Plasma Science, Faculty of Mathematics and Physics, Charles University in Prague, V Holešovičkách 2, 180 00, Prague, Czech Republic

ARTICLE INFO

Article history:
Received 10 April 2008
Received in revised form 15 May 2008
Accepted 19 May 2008
Available online 3 June 2008

Keywords:
Recombination
KrH^+
KrD^+
XeH^+
XeD^+

ABSTRACT

Recombination rate coefficients of protonated and deuterated ions KrH^+, KrD^+, XeH^+ and XeD^+ were measured using Flowing Afterglow with Langmuir Probe (FALP). Helium at 1600 Pa and at temperature 250 K was used as a buffer gas in the experiments. Kr, Xe, H_2 and D_2 were introduced to a flow tube to form the desired ions. Because of small differences in proton affinities of Kr, D_2 and H_2 mixtures of ions, KrD^+/D_3^+ and KrH^+/H_3^+ are formed in the afterglow plasma, influencing the plasma decay. To obtain a recombination rate coefficient for a particular ion, the dependencies on partial pressures of gases used in the ion formation were measured. The obtained rate coefficients, $\alpha_{KrD+}(250\,K) = (0.9 \pm 0.3) \times 10^{-8}\,cm^3\,s^{-1}$ and $\alpha_{XeD+}(250\,K) = (8 \pm 2) \times 10^{-8}\,cm^3\,s^{-1}$ are compared with $\alpha_{KrH+}(250\,K) = (2.0 \pm 0.6) \times 10^{-8}\,cm^3\,s^{-1}$ and $\alpha_{XeH+}(250\,K) = (8 \pm 2) \times 10^{-8}\,cm^3\,s^{-1}$.

© 2008 Elsevier B.V. All rights reserved.

1. Introduction

Protonated rare gas atoms, such as HeH^+, NeH^+, ArH^+, KrH^+ and XeH^+, have been studied extensively over recent years. There were several theoretical calculations [1–3] and spectroscopic studies [4,5] related to these ions. Reactions of these ions with neutral molecules and their recombination with electrons were investigated [6,7]. The recombination of these ions is important from theoretical [8], experimental and technological aspects. HeH^+, NeH^+, ArH^+ and KrH^+ ions do not have curve crossings between the ion ground state and a repulsive neutral state and they recombine slowly (with rate coefficients $\alpha(300\,K) \leq 2 \times 10^{-8}\,cm^3\,s^{-1}$) in comparison with majority of other molecular ions [7]. The recombination of HeH^+, NeH^+ and ArH^+ ions with electrons was studied in storage ring experiments [9–11]. KrH^+ and XeH^+ ions are too heavy for the existing storage ring experiments and it is not easy to study them in plasma experiments. There are few theoretical and experimental studies of KrH^+ and XeH^+ ions and their recombination with electrons [12,13]. To our knowledge, recombination rate coefficients of KrD^+ and XeD^+ ions were not measured up to now. In general, it is difficult to predict the effect when hydrogen is substituted with deuterium, it is more theoretical than experimental problem.

For example, the difference between recombination of H_3^+ and D_3^+ is very essential, the deuterium nucleus is a boson in contrast to the fermionic nucleus of hydrogen, therefore, the total nuclear-molecular symmetry differs and also it has consequences in the recombination processes. The simple statement that the rate coefficient for D_3^+ is three times smaller than the rate coefficient for H_3^+ dissociative recombination is oversimplification [14–16].

Two former FALP (Flowing Afterglow with Langmuir Probe) studies of KrH^+ and XeH^+ recombination give just the upper limits for the values of recombination rate coefficients [6,13]. In our recent FALP study [17], we obtained the following recombination rate coefficients values: $\alpha_{KrH^+}(250\,K) = (2.0 \pm 0.6) \times 10^{-8}\,cm^3\,s^{-1}$ and $\alpha_{XeH^+}(250\,K) = (8 \pm 2) \times 10^{-8}\,cm^3\,s^{-1}$. The aim of the present FALP study is to measure recombination rate coefficients for deuterated KrD^+ and XeD^+ ions and to compare their recombination with protonated equivalents.

We have recently adapted our FALP apparatus [18–20] for measurements of the recombination rate coefficients as small as $5 \times 10^{-9}\,cm^3\,s^{-1}$ [17]. In the present study, FALP is used to measure rate coefficients of KrD^+ and XeD^+ ions at 250 K. In a FALP experiment, the recombining ions are formed in the decaying afterglow plasma in helium buffer, so in principle D_2 and Kr or Xe have to be added to the carrier gas to form KrD^+ or XeD^+, respectively. In such plasmas, formation of faster recombining molecular ions (Kr_2^+, Xe_2^+, D_3^+, etc.) with recombination rate coefficients $\geq 10^{-7}\,cm^3\,s^{-1}$ or cluster ions (KrD_3^+, Kr_2D^+, H_5^+, D_5^+, etc.) with even larger recombination rate coefficients ($\geq 10^{-6}\,cm^3\,s^{-1}$) cannot be excluded from the data analysis. The influence of these ions on plasma decay and

* Corresponding author. Tel.: +420 221 912 224; fax: +420 284 685 095.
E-mail address: radek.plasil@mff.cuni.cz (R. Plasil).

1387-3806/$ – see front matter © 2008 Elsevier B.V. All rights reserved.
doi:10.1016/j.ijms.2008.05.037

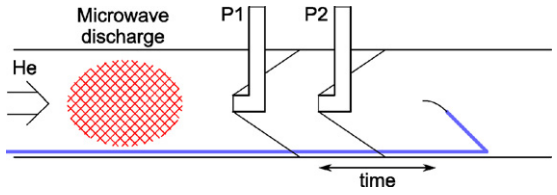

Fig. 1. The principle of FALP method. Under action of a large pump, helium buffer gas flows from the discharge region where plasma is generated along the flow tube (from left to right side in the drawing). The reactant gases are added via ports P1 and P2 to form plasma dominated by the studied ions. The Langmuir probe is movable along the flow tube from the position of port P2 up to the end of the flow tube. The relation between the decay time and the position is given by the buffer gas velocity. The decay time is counted from the position of port P2, $t_{P2} = 0$.

hence on the measured effective rate coefficient of recombination can be accounted for if the dependencies on partial pressures of reactants (Kr, D_2) are measured and the kinetics of the processes in the flowing afterglow is considered and modelled.

2. Experiments

The principle of the Flowing Afterglow method used in presented FALP experiments is described in Fig. 1, the details are given elsewhere [19,21]. In a FALP experiment, helium buffer gas flows through the glass section of the flow tube and plasma is generated by microwave discharge (~15 W). Flowing buffer gas then drives plasma into a stainless steel flow tube, where reactants can be introduced via injection ports (P1, P2). Because of high He pressure (1600 Pa), the majority of He^+ ions formed in the discharge are converted in a three-body association process to He_2^+ ions already prior to port P1. At this stage, plasma contains He_2^+ ions and electrons and also long-living helium metastables ($He(2^3S)$ and $He(2^1S)$) formed in the discharge [20,22]. In the presented experiments, the port P1 is used to add Ar in XeD^+ studies and Kr in KrD^+ studies. After addition of Ar or Kr, helium metastables are removed from the plasma by Penning ionisation and Ar^+ or Kr^+ dominated plasma is formed. When the metastables are removed the plasma rapidly relaxes. The processes of relaxation are clear and well described [21]. The parameters of the decaying plasma along the flow tube are monitored by an axially movable Langmuir probe, 7 mm long tungsten wire with diameter 18 μm.

Electron number densities are determined from the "electron saturated region" of measured probe characteristics (current to voltage) [23]. To obtain absolute values of electron densities, the probe is calibrated by measuring well-established recombination rate coefficients of O_2^+ ions [24]. In fact, the calibration just confirms accuracy of the electron density measurements based on probe theory. From the decays of the electron density (n_e) along the flow tube, recombination rate coefficients are obtained. For the very slow recombination, more advanced methods are used (see description and discussion in refs. [19,24,25]). In the experiment, helium is purified by passing through a zeolite trap cooled by liquid nitrogen to obtain impurity level below 0.1 ppm. The flow tube is cooled to 250 K to suppress partial pressure of water vapour. Under the used experimental conditions, we can monitor plasma decay over 60 ms.

3. Calculation of plasma formation and decay along the flow tube

It was already mentioned that D_2 and Kr or Xe have to be added to the flow tube to form KrD^+ or XeD^+. Formation of XeD^+ is simple: Ar is added via port P1 and Ar^+ dominated plasma is formed downstream from P1, then Xe and D_2 are added via port P2 situated ~35 ms downstream from the port P1. The reaction of Ar^+ with D_2 producing ArD^+ and D_2^+ is very fast. In opposite the reaction of Ar^+ with Xe producing Xe^+ is very slow and can be neglected in the formation process (see Table 1 for corresponding reaction rate coefficients). Since the proton affinity of Xe is considerably higher than proton affinities of Ar and D_2, the plasma will be converted from Ar^+ dominated to XeD^+ dominated in sequence of exoergic ion-molecule reactions. Calculated evolutions of ion densities along the flow tube are plotted in Fig. 2. Ions XeD^+ are not reacting further with gases in the flow tube (He/Ar/Xe/D_2). At high densities of the reactants more complex ions can be formed in three-body association processes, this will be discussed further. The densities $[Ar] \sim 1 \times 10^{13}\ cm^{-3}$ and $[D_2] = [Xe] = 5 \times 10^{12}\ cm^{-3}$ were used in the calculation. From the calculated evolutions of the ion densities, it is clear that XeD^+ dominated plasma will be formed within ≤1 ms after addition of Xe and D_2 via port P2 (see details in right panel of Fig. 2). At substantially smaller reactant densities the rates of the forming reactions will be slower and the formation region will overlap with the recombination-dominated region.

Table 1
The formation and the destruction of XeD^+; the main considered reactions and the corresponding rate coefficients used in the model

No.	Reaction	Rate coefficients [$cm^3\ s^{-1}$] or [$cm^6\ s^{-1}$]	Ref.
1	$Ar^+ + Xe \rightarrow Xe^+ + Ar$	4×10^{-13}	[26]
2	$Ar^+ + D_2 \rightarrow ArD^+ + D \rightarrow D_2^+ + Ar$	7.5×10^{-10} ArD^+ is dominant	[26]
3	$D_2^+ + Ar \rightarrow ArD^+ + D$	1.5×10^{-9}	[26]
4	$ArD^+ + D_2 \rightarrow D_3^+ + Ar$	7×10^{-10}	[26]
5	$D_2^+ + D_2 \rightarrow D_3^+ + D$	1.6×10^{-9}	[26]
6	$D_3^+ + D_2 + He \rightarrow D_5^+ + He$	1×10^{-29}	(a)
7	$D_5^+ + He \rightarrow D_3^+ + He + D_2$	1×10^{-13}	(a)
8	$ArD^+ + Xe \rightarrow XeD^+ + Ar$	5×10^{-10}	(b)
9	$D_3^+ + Xe \rightarrow XeD^+ + D_2$	1.7×10^{-9}	(c)
10	$D_3^+ + e^- \rightarrow$ products	1.3×10^{-7}	(d)
11	$D_5^+ + e^- \rightarrow$ products	3.0×10^{-6}	(a)
12	$XeD^+ + e^- \rightarrow$ products	8×10^{-8}	(d)

The data are taken from compilation of Anicich [26]. The model uses the value of the recombination rate coefficient of XeD^+ obtained in the present study. The recombination rate coefficients for XeD^+, D_3^+ and D_5^+ are taken from present measurements and from our previous experiments carried out on FALP at similar conditions (see ref. [18]). (a) The rate coefficient for the collision induced dissociation (CID) of D_5^+ in collisions with He is calculated from the known equilibrium constant and the rate coefficient of the corresponding formation process (three-body association). See also data and discussion in ref. [18]. (b) Estimation based on Langevine rate coefficient. (c) Estimation using data for reaction of H_3^+ with Xe [6]. (d) Present experiment, the value measured at 1600 Pa.

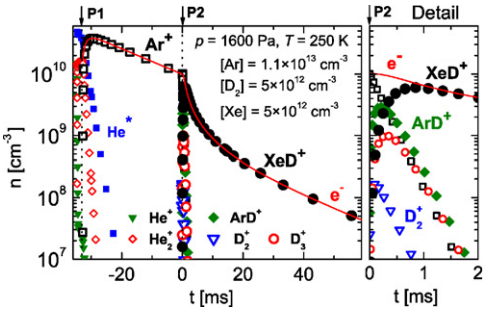

Fig. 2. The calculated plasma formation and decay along the flow tube after addition of Ar via port P1 and mixture of D_2 and Xe via port P2. The ambipolar diffusion, recombination processes and ion-molecule reactions are considered in the kinetic model. The delay due to gas mixing (*end correction*) is not considered in the model. In the right panel, the details of the evolution close to the port P2 are shown. The considered processes and corresponding rate coefficients used in the model are listed in Table 1.

The formation of KrD^+ dominated plasma requires more attention to the calculation of optimal experimental conditions. The proton affinity of Kr is only by 0.02 eV lower than the proton affinity of D_2 [27,28]. As a consequence, both ions KrD^+ and D_3^+ will be present in the flow tube downstream from the port P2 at comparable Kr and D_2 densities. The ion partial densities will be governed by reaction:

$$D_3^+ + Kr \underset{k_r}{\overset{k_f}{\rightleftarrows}} KrD^+ + D_2 \quad (1)$$

where k_f and k_r are the rate coefficients of the forward and the reverse ion-molecule reaction, respectively. In equilibrium [18,29,30], the ratio of ion densities $[D_3^+]/[KrD^+]$ is proportional to the ratio $[D_2]/[Kr]$:

$$\frac{[D_3^+]}{[KrD^+]} = \frac{K_{Eq}[D_2]}{[Kr]} \quad (2)$$

where $K_{Eq} = k_r/k_f$ is the equilibrium constant for the above reaction. The calculated evolutions of the partial ion densities along the flow tube are plotted in Fig. 3. At high densities of reactants, complex ions can be formed (will be discussed further). It is clear from the model that KrD^+ dominated plasma will be formed within <5 ms after the addition of D_2 via the port P2 (for [Kr] and $[D_2]$ higher as 5×10^{12} cm^{-3}). In the lower panel of the Fig. 3, the relative densities $f_1 = [KrD^+]/n_e$ and $f_2 = [D_3^+]/n_e$ are plotted. The conditions relevant for the measurements of KrD^+ recombination are used in the calculations. The set of differential balance equations is solved in the model and we are not using the assumption of equilibrium. The ions KrD^+ and D_3^+ will be in equilibrium if the rates of the diffusion and recombination losses (eventually other reactive losses; e.g., formation of D_5^+) can be neglected in comparison with the rates of the forward and the reverse reaction (1). This is fulfilled for conditions denoted in Fig. 3, where the evolutions of number densities are plotted. Less than 5 ms after injection of D_2, the KrD^+ and D_3^+ ions are already formed and the equilibrium is reached. In the equilibrium, the relative densities and their ratio f_2/f_1 are constant, see lower panel of Fig. 3.

4. Measurements of XeD^+ recombination rate coefficient

As already mentioned, in the XeD^+ study Ar was added via port P1 and the mixture of Xe and D_2 were added to the already cold and relaxed plasma via port P2 35 ms downstream. In every set of measurements, we measured the decay of the electron density along the flow tube in Ar^+ dominated plasma first (without addition of Xe and D_2), see decay plotted in Fig. 4. The straight line corresponding to exponential decay in the Ar^+ dominated plasma indicates losses due to pure ambipolar diffusion. The losses due to recombination of Ar^+ ions and due to reactions with impurities can be neglected in the time scale of the present experiment. Electron energy distribution function (EEDF) was measured to prove that electrons are relaxed to ~250 K [20]. Low Ar densities ($[Ar] < 10^{14}$ cm^{-3}) are used to avoid formation of fast recombining Ar_2^+ ions.

Then D_2 and Xe were added via P2 and the decay of electron density in XeD^+/D_3^+ plasma was monitored. The decay curves were measured for several Xe and D_2 densities. Examples of decay curves measured in XeD^+ and D_3^+ dominated plasmas are plotted in Fig. 4.

The role of recombination processes in early afterglow is evident from the difference between the decays of plasmas with molecular D_3^+ and XeD^+ ions and the decay of Ar^+ dominated plasma with negligible recombination. To rule out the influence of fast recombining large molecular and cluster ions formed at higher reactant densities, the measurements were carried out over broad range of Xe and deuterium densities. Used partial pressures of reactants were selected on the basis of numerical simulations. Recombination rate coefficients were obtained from the rate of the electron density decays using $1/n_e$ versus time plot [19]. The obtained rate coefficients (α) for the recombination of XeD^+ are plotted in Fig. 5. For comparison, also the measured rate coefficient for the recombination of D_3^+ is plotted. We stress here that the obtained $\alpha_{eff}(D_3^+)$ is the rate coefficient of overall deionisation process at 1600 Pa in He/Ar/D_2 plasma (see discussion in ref. [25]). The plotted $\alpha_{eff}(D_3^+)$ is not identical with the rate coefficient of binary dissociative

Table 2
Formation and destruction of KrD^+

No.	Reaction	Rate coefficients [cm^3 s^{-1}] or [cm^6 s^{-1}]	Ref.
1	$Kr^+ + D_2 \rightarrow KrD^+ + D$	1.5×10^{-10}	[26]
2	$KrD^+ + D_2 \rightarrow D_3^+ + Kr$	2.6×10^{-11}	(a)
3	$D_3^+ + Kr \rightarrow KrD^+ + D_2$	0.8×10^{-9}	(a)
4	$D_3^+ + D_2 + He \rightarrow D_5^+ + He$	1×10^{-29}	(b)
5	$KrD^+ + e^- \rightarrow Kr + D$	1.0×10^{-8}	(c)
6	$D_3^+ + e^- \rightarrow$ products	1.3×10^{-7}	(b and c)
7	$D_5^+ + e^- \rightarrow$ products	3×10^{-6}	(b)

The main considered reactions and corresponding rate coefficients used in the model. The value of the recombination rate coefficient of KrD^+ obtained in the present study is used in the model. The recombination rate coefficients for D_3^+ and D_5^+ are taken from our previous experiments carried out on FALP at similar conditions (see ref. [18]). (a) Estimation using measured rate coefficient [29] for reaction of KrH+ with H_2. A higher reduced mass of the reactants is considered. (b) See data and discussion in ref. [18]. (c) Present experiment, value measured at 1600 Pa.

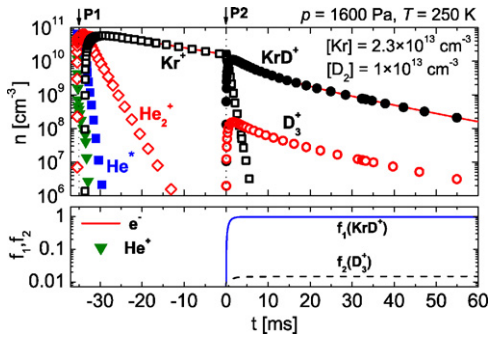

Fig. 3. The calculated plasma formation and the decay along the flow tube. Kr is added via port P1 and D_2 via port P2. The considered processes and corresponding rate coefficients used in the model are listed in Table 2. Quasi neutrality of the plasma is assumed in the calculation. In lower panel, the relative densities $f_1 = [KrD^+]/n_e$ and $f_2 = [D_3^+]/n_e$ are plotted.

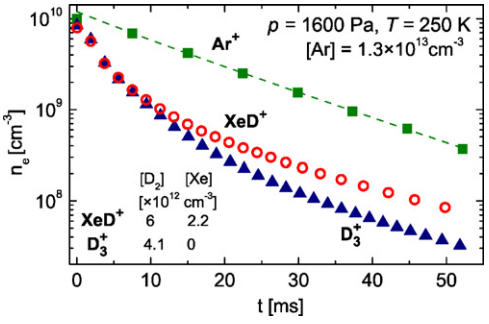

Fig. 4. The measured electron density decays along the flow tube in the Ar^+, D_3^+ and XeD^+ dominated plasmas (recalculated to the time scale). The corresponding Xe and D_2 densities are denoted. Ar density was constant for all measurements, $[Ar] = 1.3 \times 10^{13}$ cm^{-3}. The calculated formation times of D_3^+ or XeD^+ dominated plasma at used reactant densities is shorter than 1 ms (see Fig. 2), the real time of formation is given by the mixing of the gases after injection (end correction), the estimated value is ~2 ms.

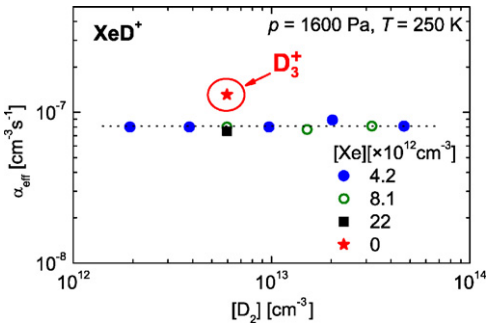

Fig. 5. The recombination rate coefficients measured in XeD^+ dominated plasma with different Xe and deuterium densities. The corresponding Xe densities are denoted. The star in the circle indicates recombination rate coefficient $\alpha_{eff}(D_3^+)$ measured in D_3^+ dominated plasma (without addition of Xe) in otherwise identical experimental conditions.

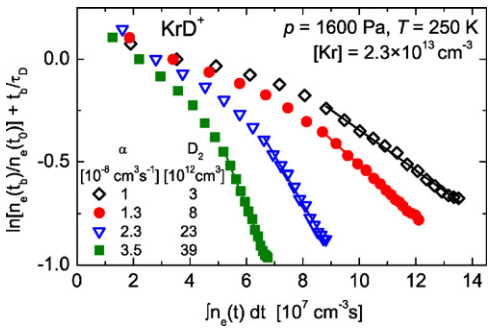

Fig. 7. Integral method: plot of $\{\ln[n_e(t_b)/n_e(t_0)] + t_b/\tau_D\}$ versus $\int n_e(t)\,dt$. Data were measured for indicated D_2 densities. Obtained effective rate coefficients corresponding to recombination in mixture of KrD^+ and D_3^+ ions are denoted in the figure.

recombination [15]. The obtained values of $\alpha_{eff}(D_3^+)$ was used in the model.

Since we obtained constant value of the recombination rate coefficient independent on Xe and deuterium density for XeD^+, we expect that the measured rate coefficient is the rate coefficient of dissociative recombination of XeD^+ ion. The obtained rate coefficient $\alpha_{XeD^+}(250\,K) = (8 \pm 2) \times 10^{-8}\,cm^3\,s^{-1}$. Using hydrogen instead of deuterium in otherwise identical experimental conditions we obtained the same value of recombination rate coefficient for XeH^+; $\alpha_{XeH^+}(250\,K) = (8 \pm 2) \times 10^{-8}\,cm^3\,s^{-1}$. This value confirms the value obtained in our previous study [17].

5. Measurements of KrD^+ recombination rate coefficient

After addition of Kr and D_2 to the flow tube (via port P1 and P2, respectively), ions KrD^+ and D_3^+ are formed in the afterglow and the plasma decay is controlled by their recombination with electrons. Decay curves measured for several densities of D_2 in KrD^+ dominated afterglow are plotted in Fig. 6. Krypton density was kept constant in the plotted set.

In the late afterglow the decay curves are nearly parallel and the decays correspond to the diffusion losses. The measured decays are very slow and the common method of rate coefficient determination from the slope of a graph of the values $1/n_e$ versus decay time is not accurate enough. For this reason, an advanced data analysis procedure has been used—"integral method" [19]. To clarify a principle of the method, we assume that KrD^+ and D_3^+ ions recombine in decaying plasma with recombination rate coefficients α_1 and α_2,

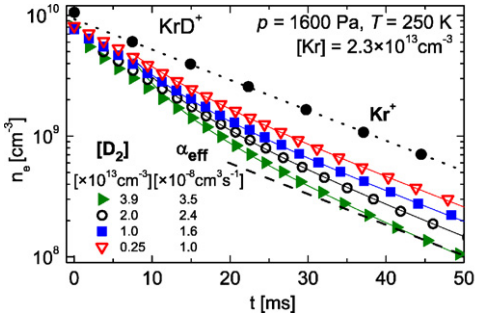

Fig. 6. The measured electron density decays in the KrD^+ dominated plasmas along the flow tube (recalculated to the time scale). The Kr and D_2 densities and the corresponding rate coefficients are denoted. The dashed straight line indicates the diffusion losses during the late afterglow in KrD^+ dominated plasma. For comparison, the decay curve measured in the Kr^+ dominated plasmas in otherwise identical conditions is also included in the plot.

respectively. Under this assumption we can write balance equation for electrons in the form:

$$\frac{dn_e}{dt} = -\alpha_1[KrD^+]n_e - \alpha_2[D_3^+]n_e - \frac{n_e}{\tau_D}$$
$$= -(\alpha_1 f_1 + \alpha_2 f_2)n_e^2 - \frac{n_e}{\tau_D}$$
$$= -\alpha_{eff} n_e^2 - \frac{n_e}{\tau_D}, \quad (3)$$

where f_1 and f_2 are partial densities of KrD^+ and D_3^+ ions, respectively. For simplicity, the diffusion term is written with characteristic diffusion time τ_D. The introduced effective rate coefficient, $\alpha_{eff} = (\alpha_1 f_1 + \alpha_2 f_2)$, will be dependent on f_1 and f_2 and on the corresponding recombination rate coefficients. In general the fractions f_1 and f_2 are dependent on the decay time. If ions are in equilibrium, then as it follows from Eq. (2), the f_1 and f_2 are constant during plasma decay (see Fig. 3) and the overall recombination can be described by constant α_{eff}. For constant values of α_{eff}, we can integrate differential Eq. (3) to the form:

$$\ln\left[\frac{n_e(t_b)}{n_e(0)}\right] + \frac{t_b}{\tau_D} = -\alpha_{eff}\int_0^{t_b} n_e(t)\,dt, \quad (4)$$

where t_b is the variable parameter scanning over all data points. If $\{\ln[n_e(t_b)/n_e(0)] + t_b/\tau_D\}$ is plotted versus $\int n_e(t)\,dt$ we should obtain line with $-\alpha_{eff}$ as a slope. In the ion formation region, α_{eff} is not constant and the plot will not give a straight line. Examples of the plots obtained with application of formula (4) are given in Fig. 7.

The fractions f_1 and f_2 can be calculated if we can rely on the value of an available equilibrium constant. It is also possible to measure α_{eff} as a function of Kr or D_2 density and to obtain α_1 as a limit for $[D_2] \to 0$ (equivalent to $f_2 \to 0$). In KrD^+ dominated plasma with only small fraction of D_3^+ ions we can write: $[KrD^+] \approx n_e$ and $f_1 \approx 1$. Then from Eq. (2) it follows: $f_2 = K_{Eq} \times [D_2]/[Kr]$. In such simple conditions, dependence of α_{eff} on deuterium density can be expressed analytically:

$$\alpha_{eff} = \alpha_1 f_1 + \alpha_2 f_2 = \alpha_1 + \alpha_2 K_{Eq}[D_2]/[Kr]$$
$$= \alpha_1 + s_{[Kr]}[D_2], \quad \text{where} \quad s_{[Kr]} = \alpha_2 K_{Eq}/[Kr] \quad (5)$$

This gives a possibility to obtain α_1 as a limit of the measured α_{eff} for $[D_2] \to 0$. In the experiment, the partial pressure of deuterium was varied and the overall recombination rate coefficient was measured as a function of this density at fixed Kr density. The measured dependence is plotted in lower panel of Fig. 8. The linear dependence is obvious. From the limit towards low $[D_2]$ we obtained $\alpha_{KrD^+} = 0.9 \times 10^{-8}\,cm^3\,s^{-1}$. The question is how the recombination process in the plasma will be influenced by presence of Kr atoms. In the measurements presented in Fig. 8, low Kr densities are deliberately used to suppress the formation

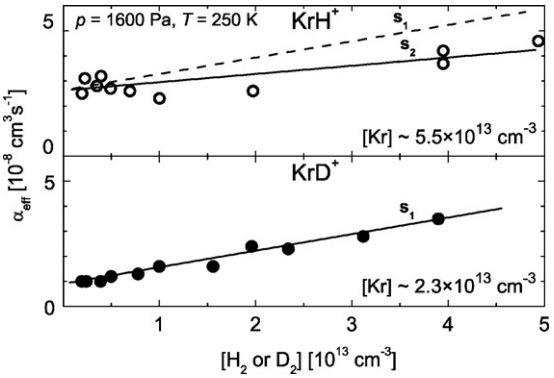

Fig. 8. Lower panel: the dependence of the effective recombination rate coefficients of KrD^+ ions on deuterium density. Indicated is the used Kr density. Full line represents linear fit (slope s_1). Upper panel: the dependence of the effective recombination rate coefficients of KrH^+ on a hydrogen density. Used Kr density is indicated. The dashed line has slope s_1 obtained for KrD^+ and the full line has slope $s_2 = s_1/1.6$ as follows from Eq. (5).

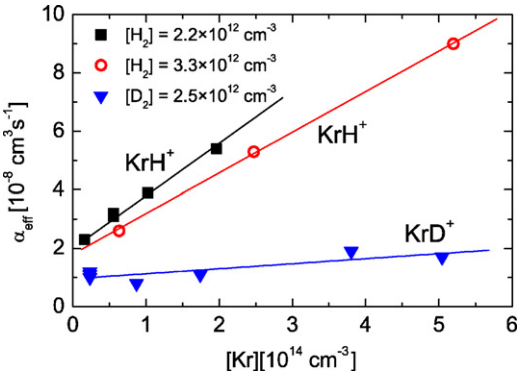

Fig. 9. The measured dependencies of the effective recombination rate coefficients on Kr density in KrH^+ and KrD^+ dominated plasmas (FALP experiment). Densities of H_2 and D_2 used here are denoted. Pressure in flow tube is 1600 Pa and temperature of helium 250 K.

of Kr containing cluster ions. In the upper panel of Fig. 8, the dependence of effective recombination rate coefficient measured for KrH^+ dominated plasma is plotted. The Kr density used in KrH^+ experiment is by factor 2.4 higher than Kr density used in KrD^+ experiment. On the other hand, the recombination rate coefficient α_2 for H_3^+ is 1.5 times higher than value for D_3^+ [16]. As a consequence, the slope (denoted as s_2) of the observed dependence in KrH^+ experiment should be in agreement with Eq. (5) by factor of 1.6 smaller than slope (s_1) measured in KrD^+ experiment. Here we are assuming that K_{Eq} does not change significantly (in comparison with the factors 2.4 and 1.5) if deuterium is used instead of hydrogen. The calculated slope s_2 is plotted in the upper panel of Fig. 8, the agreement with the measured data is very good.

If at fixed low D_2 density a Kr density will be further increased, then KrD^+ ions would be able to react with Kr in a three body association reaction:

$$KrD^+ + Kr + He \underset{k_r}{\overset{k_f}{\rightleftarrows}} Kr_2D^+ + He \qquad (6)$$

If the ions recombine with rate coefficients α_1 and α_3 for KrD^+ and Kr_2D^+, respectively, then the overall recombination rate coefficient is:

$$\alpha_{eff} = \alpha_1 f_1 + \alpha_3 f_3 = \alpha_1 + \alpha_3 K_{Eq6}[Kr], \qquad (7)$$

where K_{Eq6} is equilibrium constant for the process described by Eq. (6). The difference between formula (7) and (5) is given by the processes which are governing equilibrium. In case of equilibrium between KrD^+ and D_3^+, equilibrium is kept by binary processes. In case of equilibrium between KrD^+ and Kr_2D^+, equilibrium is kept by forward ternary association and by reverse binary collision induced dissociation. As follows from Eq. (7): for $[Kr] \to 0$ the rate coefficient $\alpha_{eff} \to \alpha_1$. The experiments were carried out for different Kr densities with constant deuterium density. The obtained effective recombination rate coefficients (α_{eff}) are plotted versus [Kr] in Fig. 9.

The used deuterium density was very low, $[D_2] = 2.5 \times 10^{12}\,cm^{-3}$, to minimise eventual influence of D_3^+ formation. In the Fig. 9, the recombination rate coefficients measured at similar conditions in KrH^+ dominated plasma are also included.

The observed dependencies on [Kr] characterise the influence of Kr on the overall recombination process in the KrH^+ and KrD^+ dominated plasmas. A linear increase for KrH^+ and KrD^+ is in agreement with the formula (7). A large difference between the observed dependencies for KrH^+ and KrD^+ is surprising and we do not have explanation for this rather strong isotope effect.

We should state here that we were just assuming that Kr_2D^+ or Kr_2H^+ ions are formed [31]; we do not have direct evidence for existence of these ions. From point of view of the measurements of recombination rate coefficient of KrH^+ and KrD^+, it is not a crucial assumption. Considering the obtained dependencies of measured effective rate coefficients on D_2, H_2 and Kr densities, we obtained the following rate coefficients for recombination of KrH^+ and KrD^+: $\alpha_{KrH^+}(250\,K) = (2.0 \pm 0.6) \times 10^{-8}\,cm^3\,s^{-1}$ and $\alpha_{KrD^+}(250\,K) = (0.9 \pm 0.3) \times 10^{-8}\,cm^3\,s^{-1}$.

6. Conclusion

Flowing Afterglow with Langmuir Probe (FALP) experiment was used to measure recombination rate coefficients of ions XeH^+ and XeD^+. The rate coefficients were measured from the decays of the electron densities in XeH^+ and XeD^+ dominated plasmas in He afterglow at 250 K. To avoid formation of other ions, low partial densities of reactant gases were used. The obtained rate coefficients are: $\alpha_{XeD^+}(250\,K) = (8 \pm 2) \times 10^{-8}\,cm^3\,s^{-1}$ and $\alpha_{XeH^+}(250\,K) = (8 \pm 2) \times 10^{-8}\,cm^3\,s^{-1}$.

The FALP was also used for the study of recombination rate coefficients of KrH^+ and KrD^+ ions. Because of small differences in proton affinities of Kr and H_2 and Kr and D_2 ions, H_3^+ and D_3^+ are formed in the decaying plasmas and their influence on measured recombination rate coefficients has to be considered. At higher Kr densities, decay of plasma is also dependent on Kr partial density and this has to be also accounted for in data analyses. By measuring effective recombination rate coefficients as a function of partial pressures of used reactants, the rate coefficients for recombination of KrH^+ and KrD^+ were obtained: $\alpha_{KrH^+}(250\,K) = (2.0 \pm 0.6) \times 10^{-8}\,cm^3\,s^{-1}$ and $\alpha_{KrD^+}(250\,K) = (0.9 \pm 0.3) \times 10^{-8}\,cm^3\,s^{-1}$.

Acknowledgements

This work is a part of the research plan MSM 0021620834 financed by the Ministry of Education of the Czech Republic and was partly supported by GACR (202/05/P095, 205/05/0390, 202/07/0495, 202/08/H057) by GAUK 53607 and GAUK 124707.

References

[1] Ch. Jungem, A.L. Roche, J. Chem. Phys. 110 (1999) 10784.
[2] I.D. Petsalakis, G. Theodorakopoulos, R.J. Buenker, J. Chem. Phys. 119 (2003) 2004.
[3] J. Ree, Y.H. Kim, H.K. Shin, J. Chem. Phys. 127 (2007) 054304.

[4] H. Odashima, F. Matsushima, A. Kozato, S. Tsunekawa, K. Takagi, H. Linnartz, J. Mol. Spectrom. 190 (1998) 107.
[5] H. Linnartz, L.R. Zink, K.M. Evenson, J. Mol. Spectrom. 184 (1997) 56.
[6] M. Geoghegant, N.G. Adams, D. Smith, J. Phys.: Atom. Mol. Opt. Phys. 24 (1991) 2589.
[7] A.I. Florescu-Mitchell, J.B.A. Mitchell, Phys. Rep.-Rev. Section Phys. Lett. 430 (2006) 277.
[8] Ch. Jungen, A.L. Roche, M. Arif, Phil. Trans. R. Soc. Lond. A 355 (1997) 1481.
[9] C. Stromholm, J. Semaniak, S. Rosen, H. Danared, S. Datz, V. Van der Zande, M. Larsson, Phys. Rev. A 54 (1996) 3086.
[10] J.B.A. Mitchell, O. Novotny, G. Angelova, J.L. LeGarrec, C. Rebrion-Rowe, A. Svendsen, L.H. Andersen, A.I. Florescu-Mitchell, A. Orel, J. Phys. B 38 (2005) 693.
[11] J.B.A. Mitchell, O. Novotny, J.L. LeGarrec, A.I. Florescu-Mitchell, C. Rebrion-Rowe, A.V. Stolyarov, M.S. Child, A. Svendsen, M.A. El Ghazaly, L.H. Andersen, J. Phys. B 38 (2005) L175.
[12] G.A. Gallup, J. Macek, J. Phys. B: Atom. Mol. Phys. 10 (9) (1977) 1601.
[13] A. Le Padellec, S. Laube, O. Sidko, C. Rebrion-Rowe, B.R. Rowe, B. Sarpal, J.B.A. Mitchell, J. Phys. B: Atom. Mol. Opt. Phys. 30 (1997) 963.
[14] S. Laube, A. Le Padellec, O. Sidko, C. Rebrion-Rowe, J.B.A. Mitchell, B.R. Rowe, J. Phys. B: Atom. Mol. Opt. Phys. 31 (1998) 2111.
[15] V. Kokoouline, C.H. Greene, Phys. Rev. A 68 (2003) 012703.
[16] J. Glosik, I. Korolov, R. Plasil, O. Novotny, T. Kotrik, P. Hlavenka, J. Varju, C.H. Greene, V. Kokoouline, I.A. Mikhaylov, Recombination of H_3^+ Ions in the Afterglow of a He-Ar-H2, arXiv:0710.2339v1 [physics.atom-ph].
[17] I. Korolov, O. Novotny, R. Plasil, P. Hlavenka, T. Kotrik, M. Tichy, P. Kudrna, J. Glosik, A. Luca, Czech. J. Phys. 56 (2006) B854.
[18] O. Novotny, R. Plasil, A. Pysanenko, I. Korolov, J. Glosik, J. Phys. B: Atom. Mol. Opt. Phys. 39 (2006) 2561.
[19] I. Korolov, O. Novotny, J. Varju, T. Kotrik, R. Plasil, M. Hejduk, J. Glosik, Contrib. Plasma Phys. 48 (2008) 521.
[20] I. Korolov, R. Plasil, T. Kotrik, P. Dohnal, O. Novotny, J. Glosik, Contrib. Plasma Phys. 48 (2008) 461.
[21] J. Glosik, G. Bano, R. Plasil, A. Luca, P. Zakouril, Int. J. Mass Spectrom. 189 (1999) 103.
[22] J. Glosik, R. Plasil, P. Zakouril, V. Poterya, J. Phys. B: Atom. Mol. Opt. Phys. 34 (2001) 2781.
[23] J.D. Swift, M.J.R. Schwar, Electrical Probes for Plasma Diagnostics, Iliffe, London, 1970.
[24] R. Plasil, J. Glosik, V. Poterya, P. Kudrna, J. Rusz, M. Tichy, A. Pysanenko, Int. J. Mass Spectrom. 218 (2002) 105.
[25] V. Poterya, J. Glosik, R. Plasil, M. Tichy, P. Kudrna, A. Pysanenko, Phys. Rev. Lett. 88 (2002) 044802.
[26] V.G. Anicich, J. Phys. Chem. Ref. Data 22 (1993).
[27] D.K. Bohme, G.I. Mackay, H.I. Schiff, J. Chem. Phys. 73 (1980) 4976.
[28] J.D. Payzant, H.I. Schiff, D.K. Bohme, J. Chem. Phys. 63 (1975) 149.
[29] P. Kebarle, in: P.B. Armentrout (Ed.), The Encyclopedia of Mass Spectrometry, vol. 1, Elsevier, Oxford, 2003.
[30] J. Glosik, P. Zakouril, V. Hanzal, V. Skalsky, Int. J. Mass Spectrom. Ion Proc. 149/150 (1995) 187.
[31] J. Lundell, H. Kunttu, J. Phys. Chem. 96 (1992) 9774.